International Journal of Technology (2017) 1: 37-47
ISSN 2086-9614

ISOTHERM STUDIES OF PYROGALLOL-IMPRINTED POLYMERS VIA PRECIPITATION POLYMERIZATION

Nor Amira Othman[1], Noor Fadilah Yusof[1], Rusli Daik[2], Faizatul Shimal Mehamod[1*]

[1]*School of Fundamental Science, Universiti Malaysia Terengganu, Kuala Nerus, Terengganu 21030, Malaysia*
[2]*Faculty of Science and Technology, Universiti Kebangsaan Malaysia, Bangi, Selangor 43600, Malaysia*

(Received: July 2016 / Revised: November 2016 / Accepted: December 2016)

ABSTRACT

Molecularly imprinted polymers (MIPs) have been the most convenient and selected methods in detection and extraction for many types of specific targets in various fields. MIPs were prepared by mixing template molecule with functional monomer in the presence of cross-linker, solvent and initiator. The selectivity of MIPs is strongly influenced by the types of functional monomer, solvent and polymerization process used. Pyrogallol-imprinted polymer (Py-IP) and non-imprinted polymer (NIP) were synthesized *via* precipitation polymerization using 4-vinylpyridine (4-VP), divinylbenzene (DVB) and azobisisobutyronitrile (AIBN) as functional monomer, cross-linker and initiator, respectively. Pyrogallol (Py) was used as a target molecule. The synthesized polymers were characterized by Fourier Transform Infrared Spectroscopy (FTIR), Scanning Electron Microscopy (SEM), and UV-Visible Spectroscopy (UV-Vis). In this study, adsorption capacity was measured by the dosage effect, contact time and selectivity study. Results showed that maximum adsorption capacity by Py-IP is above 50%. The Selectivity study shows that *k'* is >1, which indicates that Py-IP has a good selectivity towards pyrogallol. Therefore, it has a good potential to be used as an adsorbent.

Keywords: 4-vinylpyridine; Adsorption isotherm; Molecularly-imprinted polymers; Selectivity study

1. INTRODUCTION

MIPs have drawn extensive attention in the production of polymeric artificial receptors for specific molecular recognition and highly useful synthetic mimics of antibodies or enzymes. Due to their molecular recognition capability, MIPs have captured the imagination of many and their use is encouraged in numerous application areas such as in: solid-phase extraction (Tamayo et al., 2007; Lanza & Sellergren, 2001; Andersson & Schweitz, 2003); sensor (Liu et al., 2012; Uzun & Turner, 2016; Haupt & Mosbach, 2006); chromatography (Yan et al., 2007); amino acid derivatives (Scorrano et al., 2011); and drugs (Sellergren & Allender, 2005; Lulinski, 2013). Not only easy and low-cost, the synthesis of MIPs also produced polymers that are stable, versatile and resistant to a wide range of pH, solvents and temperature (Cormack & Elorza, 2004). They are normally prepared by conventional free radical polymerization (FRP), due to the tolerance of FRP for wide range of functional groups in monomers and templates, but also because conventional FRP can normally be carried out in a facile manner under mild reaction conditions.

*Corresponding author's email: fshimal@umt.edu.my, Tel: +096683822 Fax: +096683608
Permalink/DOI: https://doi.org/10.14716/ijtech.v8i1.5017

The concept of MIPs is followed Fischer's lock and key principle, in which MIPs work as a porous material that has specific molecular recognition sites, which are only suitable for a specific target molecule (Pardeshi et al., 2011). There are several principles in the process of molecular imprinting, which are as follows: (1) formation of specific complex from non-covalent bond of interactions between the template molecule(s) and the functional monomer in a polar or aprotic solvent, obtained by assembling the functional monomer around the template molecule before the polymerization process; (2) in the present of cross-linker and initiator, a rigid and porous copolymer must be obtained; and (3) the distinct cavities remain complementary to the target template molecule in size, shape and functionality after the removal of the target molecule (Yan et al., 2007; Yusof et al., 2010).

The porous structure and the surface area of MIPs can be defined from several factors, including functional monomers, cross-linkers, solvent and the synthesis conditions (Santora et al., 2001; Okay, 2000). It also has been stated that the selectivity of MIPs are strongly influenced by the types of functional monomer(s) used. There are many types of functional monomers that have been used as reported in the preparation of MIPs (Zhang et al., 2003; Yilmaz et al., 1999; Urraca et al., 2008). Due to the wide range of templates used, the number of functional monomers are also various (Cormack & Elorza, 2004; Mehamod et al., 2015). There are different types of functional monomers used in the imprinting field such as acidic, basic and neutral. The most selected types of functional monomers used are the acidic ones, for example acrylic acid and methacrylic acid. Acidic functional monomers are able to establish stronger hydrogen bonds with polar solvent, such as acetonitrile. However, basic functional monomers were reported to be interacting strongly with some template molecules and this interaction contributed to the bleeding template phenomenon (Mayes & Whitcombe, 2005). Therefore, it was reported less often about the proof of the interaction between a basic functional monomer and a polar solvent.

4-vinylpyridine (4-VP) is a basic type of functional monomer. 4-VP has interesting properties that appear from the vinyl and benzene ring with a nitrogen atom. It is chemically modifiable and offers lots of advantages due to the nitrogen atom. Research has been reported that 4-VP shows antimicrobial effects of quaternized by modifying 4-VP with different agents, such as different alkyl chain and groups of $–NH_2$ and OH (Tiller et al., 2001; Tiller et al., 2002). Naturally, 4-VP is used for vast applications, not only in the MIPs field (Sahiner & Yasar, 2013).

In this study, molecularly imprinted polymer (MIP) and non-imprinted polymer (NIP) are prepared *via* precipitation polymerization, using pyrogallol (Py) and divinylbenzene (DVB) as template and cross-linker, respectively. 4-VP has been selected to be the functional monomer, due to its properties to form hydrogen bonding with the template molecule. The synthesized polymers were characterized by Fourier Transform Infrared Spectroscopy (FTIR) and Scanning Electron Microscope (SEM). Binding capabilities were studied *via* UV-Vis Spectrophotometer readings in terms of dosage effect, contact time, different concentration and selectivity study.

2. EXPERIMENTAL SETUP

2.1. Chemicals

Pyrogallol (Py), 4-vinylpyridine (4-VP), divinylbenzene (DVB), and azobisisobutyronitrile (AIBN) were obtained from Sigma Aldrich. Other chemicals of reagents were purchased from Merck. All chemicals were purified and AIBN was re-crystallized by methanol before being used.

2.2. Synthesis of Pyrogallol-Imprinted Polymer (Py-IP) and NIP

In general, Py-IP was prepared *via* precipitation polymerization method by dissolving 1.37 mmol of pyrogallol in 100 ml of acetonitrile. This was followed by the addition of 4.11 mmol of 4-VP, and 27.40 mmol of DVB-80. Finally 1.78 mmol of AIBN was added. The solution was purged with nitrogen gas for 30 minutes in an ice-bath. The bottle was placed on a Stovall flat-bed roller. The temperature was ramped from room temperature to 60°C over a period of approximately 2 hours and then kept constant at 60°C for 48 hours. After 48 hours, the solution was cooled to room temperature. The obtained precipitate was filtered and rinsed with methanol. Then the sample was washed using a soxhlet extraction method with a solution of methanol and acetic acid (9/1: v/v). The polymer was transferred to a pre-weighed vial and dried to a constant mass at 40°C for 24 hours. The NIP was prepared in the same manner, but in the absence of a template.

2.3. Characterizations

The size and shape of samples obtained were observed under Scanning Electron Microscopy (SEM) model JEOL JSM-6360LA. The functional groups of the samples obtained were determined by Fourier transform infrared spectroscopy (FTIR) model Perkin Elmer Spectrophotometer Spectrum GX.

2.4. Binding Studies

The analysis of binding studies was carried out using UV-Vis Spectrophotometer, Shimadzu. The applicability of isotherm models used was studied by obtaining the highest correlation coefficient, R^2 values in the isotherm plot.

2.4.1. Isotherm study

5 ml of target solution was placed in contact with 5 different dosage of adsorbent (2, 4, 6, 8, and 10 mg) and measured.

2.4.2. Kinetic study

At equilibrium dosage (8 mg) from the isotherm study obtained, the adsorbent is placed in contact with 5 ml of target solution. The kinetic study was measured by the interval time of 5, 10, 15, 30, 60, 120 and 140 min.

2.4.3. Selectivity study

In order to measure the selectivity of the imprinted polymer, a compound with most similar structure with pyrogallol was studied. In this study, Gallic acid had been chosen at 5 ml of 10 ppm for each compound, which was added together in 10 ml centrifuge. Then 8 mg of Py-IP was added into the solution. The mixture was centrifuged for 60 min. After 60 minutes of contact time, the solution was filtered and measured.

3. RESULTS

3.1. Synthesis of Pyrogallol-imprinted Polymer (Py-IP) and NIP

Py-IP and NIP were successfully synthesized using precipitation polymerization. From the polymerization, spherical polymer beads were obtained and these were free from stabilizer or surfactant. This is the advantage of using precipitation polymerization. Other than that, this method does not require post-processing steps. However, the isolated yields of products were moderate to good, with Py-IP (28%) being higher yield compared to NIP (20%).

3.2. Characterization

Figure 1 shows SEM images of Py-IP and NIP. Both images show the morphology of the synthesized polymers, which were in the form of spherical beads. The Py-IP sample obtained was more homogeneous compared to the NIP, which was heterogeneous in shape. The particles ranging in diameter from ~9 μm (Py-IP) to 3 μm (NIP) were obtained.

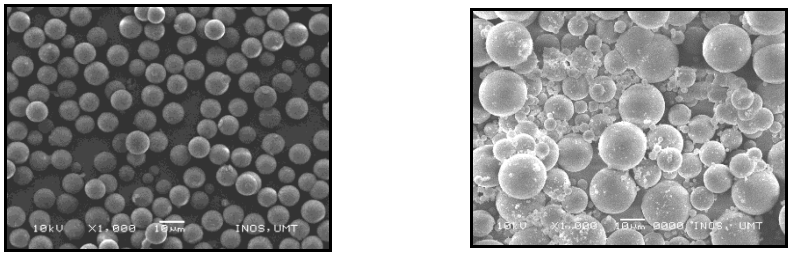

(a) (b)

Figure 1 SEM image of: (a) Py-IP; (b) NIP

The Py-IP and NIP were characterized by FTIR Spectroscopy. Unsurprisingly, the images are similar, given that the polymers have rather similar FTIR spectra as shown in Figure 2. However, there was a slight difference between the FTIR spectrum of the Py-IP and the NIP. This is due to the presence of the template in the Py-IP spectrum.

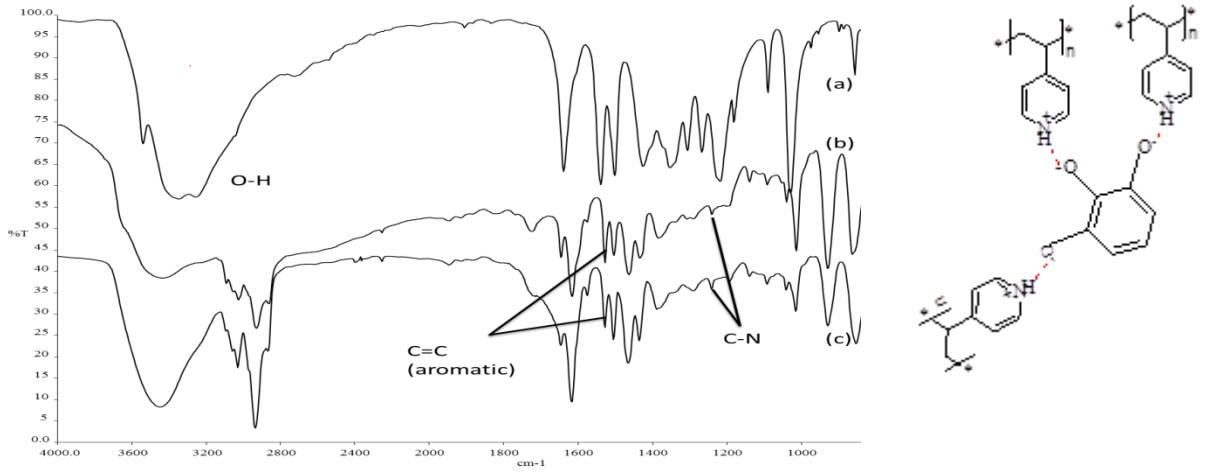

Figure 2 FTIR spectra for: (a) Py; (b) Py-IP; (c) NIP and proposed schematic interaction of Template-Monomers

According to the FTIR spectra, several active functional groups from the pyrogallol, Py-IP and NIP were detected. The backbone for pyrogallol (a) is determined by the presence of O-H stretching (3399 cm^{-1}), which indicates the hydroxyl group of phenol. It showed a broad and strong peak. Meanwhile, for both the Py-IP (b) and the NIP (c) cases, an identical spectra is shown, due to same functional monomer used. The 4-VP functional monomer backbone is indicated by the presence of both aromatic C=C bending and C-N stretching. It has been reported that aromatic C=C and C-N bonds usually appeared at 1510–1450 cm^{-1} and 1250–1210 cm^{-1}, respectively (Coates, 2000). However, there was a slight shift of the C-N bond in the Py-IP (b) spectrum compared to the C-N bond on the NIP spectrum, due to the interaction with pyrogallol.

3.3. Binding Studies

3.3.1. Isotherm study

The dependence of Py-IP and NIP on the dosage of sorbent was studied by varying the amount of dosage from 2, 4, 6, 8 and 10 mg, respectively. Results show that Py-IP adsorbs more target molecules when compared to NIP. Py-IP achieved equilibrium at 6 mg and NIP at 8 mg, as shown in Figure 3. Py-IP adsorbed up to 50% of target molecule, meanwhile NIP was able to adsorb only up to 30% of the target molecule.

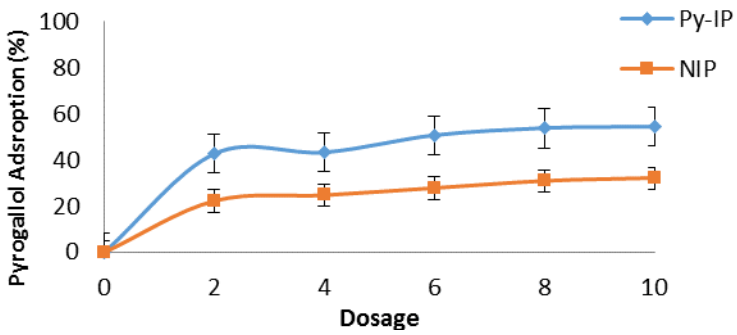

Figure 3 Pyrogallol adsorption by NIP and Py-IP

To understand the mechanism of the polymers adsorption, equilibrium data from the respective effects of the dosage was applied on three types of isotherm models. Langmuir, Freundlich and Scatchard isotherm models were used to indicate the mechanism of adsorption by both Py-IP and NIP. In general, Langmuir is used to determine the homogeneity of the surface and the sorption rate has no relation towards the amount of the sorbate molecule being used (Lampman et al., 2010.). Scatchard is one of Langmuir isotherm linear regressions, which also explains the homogeneity of the surface of the adsorbate. Meanwhile, Freundlich described the heterogeneous characteristics of the surface and the energy used for the sorption by the sorbate on the different levels of the surface (García-Calzón & Díaz-García, 2006; Mizaikoff & Wei, 2007; Matsui et al., 1995). The Langmuir, Freundlich and Scatchard isotherm models can be represented by Equation 1, Equation 2 and Equation 3, respectively (Gupta & Ali, 2000; Bolster & Hornberger, 2007; Chen, 2015).

$$(l/q_e) = (l/Q_0) + (l/bQ_0)(l/C_e) \quad (1)$$

$$\log q_e = \log K_f + (l/n) \log C_e \quad (2)$$

$$Q_e/C_e = Q_0/K_D - (1/K_D)Q_e \quad (3)$$

Table 1 shows that Py-IP (0.9994) and NIP (0.9996) followed the Scatchard isotherm by obtaining a higher R^2 value. Q_0 is related to the adsorption capacity for Scatchard isotherm. K_D is the constant value for Scatchard isotherm that is related to the affinity constant for binding and energy sorption (Khairi et al., 2015).

Table 1 Langmuir and Freundlich constants for adsorption isotherm

Samples	Langmuir			Freundlich			Scatchard		
	R^2	Q_o	*B*	R^2	K_f	*n*	R^2	Q_{max}	K_D
Py-IP	0.7606	1.49	0.14	0.9605	262.72	0.24	0.9994	1.27E-04	8.77
NIP	0.9579	0.36	0.11	0.9194	22.19	0.13	0.9996	3.51E-04	6.37

3.3.2. Kinetic study

The kinetic study was carried out by allowing Py-IP and NIP in contact with target molecule at interval times ranging from 0, 5, 10, 15, 30, 60, 120 and 140 min, respectively. Figure 4 shows the effect of time towards the adsorption of pyrogallol by Py-IP and NIP. Adsorption of pyrogallol by Py-IP achieved equilibrium at 60 minutes and NIP was achieved as early as 40 minutes. At the equilibrium point, Py-IP and NIP adsorbed up to 50% and 30% of target molecules, respectively.

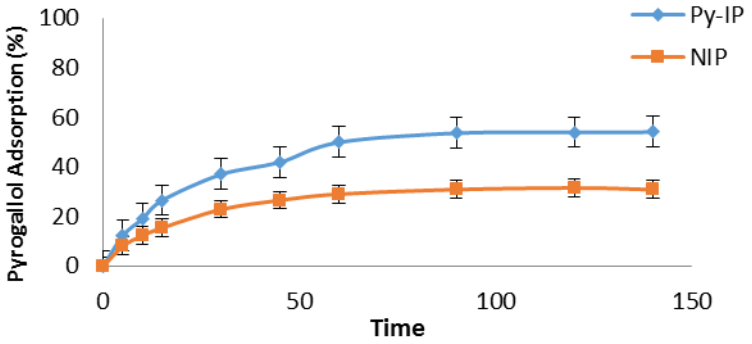

Figure 4 Effect of contact time on adsorption pyrogallol by Py-IP and NIP

To understand the behavior of adsorption mechanism, the data from kinetic adsorption was analyzed using pseudo-first-order and pseudo-second-order models. The pseudo-first-order and pseudo-second-order can be represented by Equation 4 and Equation 5 (Liu et al., 2004).

$$\log (q_e - q_t) = \log q_e - (k_1/2.303)t \quad (4)$$

$$l/q_t = l/k_s q_e^2 + t/q_e \quad (5)$$

The adsorption kinetic constants for the pseudo-first-order and pseudo-second-order are listed in Table 2. Results showed that the R^2 of the pseudo-second-order for both Py-IP (0.9952) and NIP (0.9932) was higher than the R^2 of the pseudo-first-order. K_1 and K_2 indicate the adsorption rate of the pseudo-first-order and the pseudo-second-order, respectively. These results showed that the adsorption rates of Py-IP and NIP, respectively were faster for the pseudo-second-order compared to the pseudo-first-order.

Table 2 Kinetic constants for Py-IP and NIP

Samples	Pseudo-First Order			Pseudo-Second Order		
	R^2	q_e	K_1	R^2	q_e	K_2
Py-IP	0.7452	1.6873	0.3390	0.9952	3.9401	0.0470
NIP	0.0559	1.2416	6.4484×10^3	0.9932	2.1556	0.0498

3.3.3. Selectivity study

The Selectivity of Py-IP and NIP towards pyrogallol was studied in order to estimate the effect of imprinting factor. Gallic acid (GA) was selected to be used as analogue template to pyrogallol due to the similarity properties. Figure 5 shows that the adsorption of pyrogallol by Py-IP was higher than NIP. This was due to the complementary binding sites in Py-IP compared to NIP. However, the adsorption of GA by NIP was higher than Py-IP, due to the non-existence of an imprinting site inside the polymer matrix.

The Selectivity studies involved the distribution and coefficient of GA with pyrogallol, which can be calculated by the following Equation 6, where K_d is the distribution coefficient.

$$K_d = \frac{(C_i - C_f)}{M} \times V \quad (6)$$

Selectivity coefficient (k) can be calculated by the following Equation 7:

$$k = \frac{K_d\ (Py)}{K_d\ (GA)} \quad (7)$$

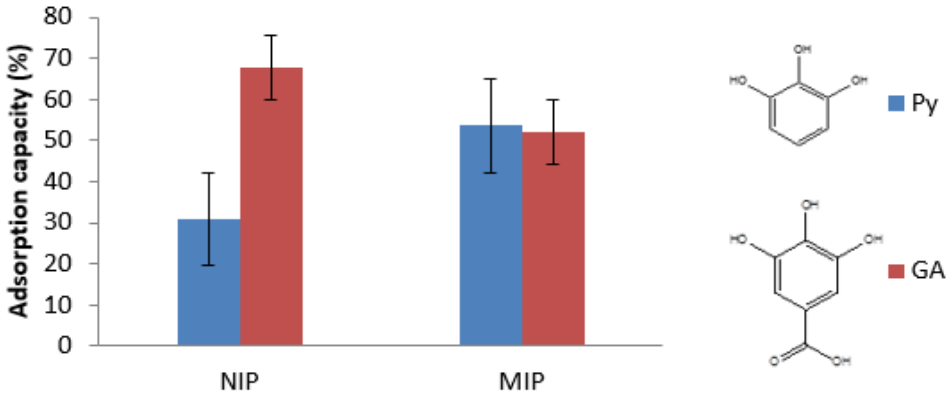

Figure 5 Selectivity study by Py-IP and NIP

The relative selectivity studies can be calculated from selectivity coefficient by the following Equation 8:

$$k' = \frac{k_{imprinted}}{k_{control}} \tag{8}$$

Table 3 shows the summary of K_d, k and k' for the selectivity study between GA and pyrogallol. The k' value for Py-IP is 2.2617, which represents a good selectivity towards pyrogallol (Yusof et al., 2013; Liu et al., 2004). This shows that the binding cavities has successfully been imprinted in Py-IP.

Table 3 Selectivity study constant for Py-IP and NIP

Target Molecule	K_d NIP	K_d Py-IP	k_{nip}	$k_{Py\text{-}IP}$	k'
Pyrogallol (Py)	1.9290	3.3565	0.4552	1.0296	2.2617
Gallic Acid (GA)	4.2374	3.2600			

4. DISCUSSION

The main objective of this research was to study the binding capacity of Py-IP and NIP using 4-VP as a functional monomer in a polar solvent under precipitation polymerization. The yield obtained for the synthesized polymers were low. This might be due to the types of the functional monomer used. As discussed earlier, functional monomer is one of the components which responsible for the binding interactions in the imprinted binding sites (Cormack & Elorza, 2004). The interaction and the stoichiometric ratio between template and monomers are important parts because the strength of this interaction reflects the performance of MIPs. However in this study, free radical polymerization was used in excess monomer which contributed to the lower yield of product.

Results from precipitation polymerization process yielded spherical beads. The uniformity of the beads obtained was due to the influence of toluene in the acetonitrile-toluene mixture (Pardeshi et al., 2014). SEM results also show the difference of diameter between Py-IP and NIP, due to the presence of the template that can affect the formation of the imprinted polymer (Farrington et al., 2006). Particles with size range of 9 µm (Py-IP) and 3 µm (NIP) were obtained. The SEM micrographs were revealed that Py-IP with imprinting effect of pyrogallol showed relatively rougher microstructure. The rougher surface was attributed to the binding occurred, resulting in cavities when the template was removed (González et al., 2006). A few

similar observations were also reported, which were attributed to the differences in surface morphology between the imprinted polymer and the NIPs (Ahamed et al., 2013; Santos et al., 2014; Sikiti et al., 2014) studied by SEM. Next, the FTIR studies showed that both Py-IP and NIP had similar backbone, due to the similar functional monomer used. According to the FTIR spectra, peaks that indicated the backbone of the template (3399 cm^{-1}) do not exist in the Py-IP spectrum. This suggests that the template was completely removed from the polymer complex.

Binding studies of Py-IP and NIP were obtained from the experimental work on the different dosage, contact time and selectivity variables. Results from the different dosages studied showed that Py-IP achieved equilibrium at 6 mg and NIP achieved equilibrium at 8 mg, respectively. Equilibrium was achieved due to the high complimentarity between the target molecule and binding sites in the polymers. The equilibrium stage was established due to the resistance of the adsorption into the deep cavities when the surface cavities were occupied by target molecule (Kan et al., 2008). As from the result, the NIP achieved equilibrium earlier than the Py-IP. This result concluded that, the NIP had no cavities and was occupied with target molecules faster. In order to understand the mechanism of the polymers' adsorption, the adsorption isotherm was applied. Results showed that Py-IP and NIP fitted the Scatchard isotherm. Since the Scatchard isotherm is synonymous with the Langmuir Type IV model, this explained that the relationship between the number of active sites of the adsorbent surface and the analyte concentration. From the result, Py-IP had higher value of K_D, which indicates the efficient adsorption capacity of the polymer and the value of $n < 1$ indicates that the chemical process occurred in different levels of the Py-IP surface (García-Calzón & Díaz-García, 2006). In some studies, the Scatchard plot yields a straight line, which suggested that the polymers represented only one type of binding site (Wu et al., 2008).

The kinetic study was calculated from the effect of contact time on pyrogallol adsorption by NIP and Py-IP, respectively. From the results, NIP achieved equilibrium earlier when compared to Py-IP. This is due to the non-existence of binding cavities in the NIP. To understand the behavior of the adsorption mechanism, the kinetic study was calculated using a pseudo-first-order and pseudo-second-order method. Results showed that NIP and Py-IP followed the pseudo-second-order. As an explaination, the pseudo-second-order explains the rate-limiting step at the surface involves chemisorption. Chemisorption explains that the removal from the solution is due to the physicochemical interaction between the two phases (Robati, 2013). Chemisorption is an adsorption process, which is based on chemical reactions between the adsorbate and the adsorbent's surface. This process involves the valence force that allows the exchange or sharing of electrons to occur (Vimonses et al., 2009). From this research, the pyrogallol molecule can interact with the imprinted sites in the polymer matrices during the molecular recognition stage.

Selectivity of Py-IP and NIP was studied in comparison to GA, which has similar properties to Py. It was determined by the value of relative selectivity (*k'*). The value of *k'* must >1 to consider the imprinted polymer to be acceptable and to have a good selectivity towards the target molecule (Yusof et al., 2013; Liu et al., 2004). Results showed that the value of *k'* for Py-IP was >1, which indicated that Py-IP was successfully imprinted and had a good selectivity towards Py.

5. CONCLUSION

As a conclusion, Py-IP and NIP was successfully synthesized *via* precipitation polymerization and spherical polymers beads were obtained. Binding properties for Py-IP and NIP were evaluated by adsorption isotherm studies. As a result, maximum adsorption capacity obtained for Py-IP and NIP was up to 50% and 30%, respectively. Py-IP achieved equilibrium at 60

minutes while NIP achieved equilibrium earlier, at 40 minutes of adsorption time, due to the absences of cavities. From the experimental data, Py-IP and NIP fitted the Scatchard isotherm and both obeyed the properties of a pseudo-second-order. The Selectivity study showed that the value of the *k'* is >1, which indicated that Py-IP had a good selectivity towards pyrogallol and was successfully imprinted.

6. ACKNOWLEDGEMENT

We would like to thank for Ministry of Education Malaysia for project funding supported and Universiti Malaysia Terengganu for supporting the facilities.

7. REFERENCES

Ahamed, M., Mbianda, X., Mulaba-Bafubiandi, A., Marjanovic, L., 2013. Selective Extraction of Gold (III) from Metal Chloride Mixtures Using Ethylenediamine N-(2-(1-imidazolyl)ethyl) chitosanion-imprinted Polymer. *Hydrometallurgy*, Volume 140, pp. 1–13

Andersson, L.I., Schweitz, L., 2003. Solid-phase Extraction on Molecularly Imprinted Polymers. *Hanbook of Analysis*, Volume 4, pp. 45–71

Bolster, C.H., Homberger, G.M., 2007. On the Use of Langmuir Equations. *Soil Science Society of America Journal*. Volume 71(6), pp. 1796–1806

Chen, X., 2015. Modeling of Experimental Adsorption Isotherm Data. *Information*, Volume 6(1), pp. 14–22

Coates, J., 2000. Interpretation of Infrared Spectra, A Practical Approach. *Encyclopedia of Analytical Chemistry*, pp. 10815–10837

Cormack, P.A.G., Elorza, M.Z., 2004. Review-molecularly Imprinted Polymers: Synthesis and Characterization. *Journal Chromatography*, Volume 804, pp. 173–182

Farrington, K., Magner, E., Regan, F., 2006. Predicting the Performance of Molecularly Imprinted Polymer: Selective Extraction of Caffeine by Molecularly Imprinted Solid Phase Extraction. *Analytica Chimica Acta*, Volume 566, pp. 60–68

García-Calzón, J.A., Díaz-García, M.E., 2006. Characterization of Binding Sites in Molecularly Imprinted Polymers. *Sensor and Actuators*, Volume 123, pp. 1180–1194

González, G.P., Hernando, P.F., Alegria, J.D. 2006. A Morphological Study of Molecularly Imprinted Polymers using the Scanning Electron Microscope. *Analytica Chimica Acta*, Volume 557(1), pp. 179–183

Gupta, V.K., Ali, I., 2000. Utilisation of Bagasse Fly Ash (a Sugar Industry Waste) for the Removal of Copper and Zinc from Wastewater. *Journal Purification Technology*, Volume 18, pp. 131–140

Haupt, K., Mosbach, K., 2006. Molecularly Imprinted Polymers and their Use in Biomimetic Sensors. *Chemical Reviews*, Volume 100, pp. 2495–2504

Kan, X., Zhoa, Q., Zhang, Z., Wang, Z., Zhu, J.J., 2008. Molecularly Imprinted Polymers Microsphere Prepared by Precipitation Polymerization for Hydroquinone Recognition. *Talanta*, Volume 75, pp. 22–26

Khairi, N.A.S., Yusof, N.A., Abdullah, A.H., Mohammad, F., 2015. Removal of Toxic Mercury from Petroleum Oil by Newly Synthesized Molecularly-imprinted Polymer. *International Journal of Molecular Sciences*. Volume 16(5), pp. 10562–10577

Lampman, G.M., Pavia, D.L., Kriz, G.S., Vyvyan, J.R., 2010. *Introduction to Spectroscopy, 4th Edition*. USA: Brooks/Cole

Lanza, F., Sellergren, B. 2001. Molecularly Imprinted Extraction Materials for Highly Selective Sample Cleanup and Analyte Enrichment. *Advanced Chromatoghraphy*, Volume 41, pp. 137–173

Liu, Y., Chang, X., Wang, S., Guo, Y., Din, B., Meng, G., 2004. Solid-phase Extraction and Preconcentration of Cadmium(II) in Aqueous Solution with Cd(II)-imprinted Resin (poly-Cd(II)-DAAB-VP) Packed Columns. *Analytica Chimica Acta*, Volume 519, pp. 173–179

Liu, Y., Zhu, L., Zhang, Y., Tang, H., 2012. Electrochemical Sensoring of 2,4 Dinitrophenol by Using Composites of Grapheme Oxide with Surface Molecular Imprinted Polymer, Sensors and Actuators B. *Chemica*, Volume 171–172, pp. 1151–1158

Lulinski, P., 2013. Molecularly Imprinted Polymers as the Future Drug Delivery Devices. *Acta Polonia Pharmaceutica-Drug Research*, Volume 70(4), pp. 601–609

Matsui, J., Miyoshi, Y., Doblhoff-Dier, O., Takeuchi, T. 1995. A Molecularly Imprinted Synthetic Polymer Receptor Selective for Atrazine. *Analytica Chemica Acta*, Volume 67(23), pp. 4404–4408

Mayes, A.G., Whitcombe, M.J., 2005. Synthetic Strategies for the Generation of Molecularly Imprinted Organic Polymers. *Advanced Drug Delivery Review*, Volume 571, pp. 1742–1778

Mehamod, F.S., KuBulat, K., Yusof, N.F., Othman, N.A., 2015. The Development of Molecular Imprinting Technology for Caffeine Extraction. *International Journal of Technology*. Volume 6(4), pp. 546–554

Mizaikoff, B., Wei, S. 2007. Binding Site Characterization of 17β-estradiol Imprinted Polymers. *Biosensor and Bioelectronics*, Volume 23, pp. 201–209

Okay, O., 2000. Macroporous Copolymer Network. *Progress in Polymer Science*, Volume 25(6), pp. 771–779

Pardeshi, S., Kumar, A., Dhodapkar, R. 2011. Molecular Imprinting: Mimiking Molecular Receptors for Antioxidants. *Material Science Forum*, Volume 675(677), pp. 512–520

Pardeshi, S., Kumar, A., Dhodapkar, R. 2014. Molecularly Imprinted Microspheres and Nanoparticles Prepared Using Precipitation Polymerisation Method for Selective Extraction of Gallic Acid from Emblica Officinalis. *Food Chemistry*, Volume 146, pp. 385–393

Robati, D., 2013. Pseudo-second-order Kinetic Equations for Modeling Adsorption Systems for Removal of Lead Ions using Multi-walled Carbon Nanotube. *Journal of Nanostructure in Chemistry*, Volume 3, pp. 55–60

Sahiner, N., Yasar, A.O., 2013. The Generation of Desired Functional Group on Poly(4-vinyl Pyridine) Particles by Post-modification Technique for Antimicrobial and Environment Application. *Journal of Colloid and Interface Science*, Volume 402, pp. 327–333

Santora, B.P., Gagnè, M.R., Moloy, K.G., Radu, N.S., 2001. Porogen and Crosslinking Effects on the Surface Area, Pore Volume Distribution, and Morphology of Macroporous Polymers Obtained by Bulk Mpolymerization. *Macromolecules*, Volume 34, pp. 658–666

Santos, Q.O., Bezerra, M.A., Lima, G.D.F., Diniz, K.M., Segatelli, M.G., Germiniano, T.O., Tarley, C.R., 2014. Synthesis, Characterization and Application of Ion Imprinted Poly(vinylimidazole) for Zinc Ion Extraction/Preconcentration with FAAS Determination. *Química Nova*, Volume 37(1), pp. 63–68

Sellergren, B., Allender, C.J., 2005. Molecularly Imprinted Polymers: A Bridge to Advanced Drug Delivery. *Advanced Drug Delivery Reviews*, Volume 57, pp. 1733–1741

Sikiti, P., Msagati, T.A., Mamba, B.B., Mishra, A.K., 2014. Synthesis and Characterization of Molecularly Imprinted Polymers for the Remediation of PCBs and Dioxins in Aqueous Environments. *Journal of Environmental Health Science and Engineering*, Volume 12(82), pp. 1–8

Scorrano, S., Lucia, M., Roberta, D.S., Guiseppe, V., 2011. Synthesis of Molecularly-imprinted Polymers for Amino Acid Derivatives by Using Different Functional Monomers. *International Journal Molecule Sciences*, Volume 12(3), pp. 1735–1743

Tamayo, F.G., Turiel, E., Martin-Esteban, A., 2007. Molecularly Imprinted Polymers for Solid-phase Extraction and Solid-phase Microextraction: Recent Developments and Future Trends. *Journal of Chromatography A*, Volume 1152, pp. 32–40

Tiller, J.C., Lee, S.B., Lewis, K., Klibanov, A.M., 2002. Polymer Surface Derivatized with Poly(Vinyl-N-hexyl pyridium) Kill Airborne and Waterborne Bacteria. *Biotechnology and Bioengineering*, Volume 79(4), pp. 465–471

Tiller, J.C., Liao, C.J., Lewis, K., Klibanov, A.M., Natl, P., 2001. Designing Surfaces that Kill Bacteria on Contact. *Proc Natl Acad Sci U S A*, Volume 98(11), pp. 5981–5985

Urraca, J.L., Carbajo, M.C., Torralvo, M.J., Gonzales-Vasquez, J., Orellana, G., Moreno-Bondi M.C., 2008. Effect of the Template and Functional Monomer on the Textural Properties of Molecularly Imprinted Polymers. *Biosensors and Bioelectronics*, Volume 24, pp. 155–161

Uzun, L., Turner, A.P.F., 2016. Molecularly-imprinted Polymer Sensors: Realising their Potential. *Biosensors and Bioelectronics*, Volume 76, pp. 131–144

Vimonses, V., Lei, S., Jin, B., Chow, C.W., Saint, C., 2009. Kinetic Study and Equilibrium Isotherm Analysis of Congo Red Adsorption by Clay Materials. *Chemical Engineering Journal*, Volume 148(2), pp. 354–364

Wu, Y., Zhang, S., Guo, X., Huang, H. 2008. Adsorption of Chromium (III) on Liginin. *Bioresource Technology*, Volume 99(16), pp. 7709–7715

Yan, S., Gao, Z., Cheng, Y., Zhou, H., Wang, H., 2007. Characterization and Quality Assessment of Binding Properties of Malachite Green Molecularly-imprinted Polymers, Prepared by Precipitation Polymerization in Acetonitrile. *Dyes and Pigments*, Volume 74, pp. 572–577

Yilmaz, E., Mosbach, K., Haupt, K., 1999. Influence of Functional and Cross-linking Monomers and the Amount of Template on the Performance of Molecularly Imprinted Polymers in Binding Assays. *Analytical Communications*, Volume 36, pp. 167–170

Yusof, N.A., Beyan, A., Haron, M.D., 2010. Synthesis and Characterization of Molecularly Imprinted Polymer for Pb2+ Uptake using 2-vinylpyridine as the Complexing Monomer. *Sains Malaysiana*, Volume 35(5), pp. 829–835

Yusof, N.A., Rahman, S.K., Hussein, M.Z., Ibrahim, N.A. 2013. Preparation and Characterization of Molecularly Imprinted Polymer as SPE Sorbent for Melamine Isolation. *Polymer*, Volume 5, pp. 1215–1228

Zhang, L., Cheng, G., Fu, C., Liu, X., 2003. Tyrosine Imprinted Polymer Beads with Different Functional Monomers via Seed Swelling and Suspension Polymerization. *Polymer Engineering and Science*, Volume 4, pp. 965–974